UMSHA Press

AJMB
Avicenna Journal of Medical Biochemistry

Avicenna J Med Biochem, 2024; 12(2):98-105. doi:10.34172/ajmb.2518

http://ajmb.umsha.ac.ir

Original Article

Investigating the Antioxidant, Antibacterial, and Anti-biofilm Effects of Cerium Oxide Nanoparticles Synthesized by Alginate

Soudabe Mousaiyan[1], Javad Baharara[1], Ali Es-haghi[1*], Ehsan Yousefi[2]

[1]Department of Biology, Mashhad Branch, Islamic Azad University, Mashhad, Iran
[2]Department of Cell and Molecular Biology & Microbiology, Faculty of Biological Science and Technology, University of Isfahan, Isfahan, Iran

Article history:
Received: July 2, 2024
Revised: September 2, 2024
Accepted: September 8, 2024
ePublished: December 31, 2024

***Corresponding author:**
Ali Es-haghi,
Email: ashaghi@gmail.com

Abstract

Background: In recent years, nanoparticles have gained increasing popularity over traditional physicochemical methods for fighting pathogenic microorganisms. Due to their unique properties, cerium oxide nanoparticles (CeO_2 NPs) have recently emerged as a promising candidate for biomedical applications.

Objectives: This study aimed to investigate the antibacterial effects of CeO_2 NPs prepared using alginate, following the disc diffusion method.

Methods: For this purpose, four bacterial strains were used in this study: two Gram-positive [*Bacillus subtilis* (PTCC 1365) and *Staphylococcus aureus* ATCC 25923] and two Gram-negative [*Escherichia coli* ATCC 25922 and *Pseudomonas aeruginosa* ATCC 9027]. The minimum inhibitory concentration (MIC) and minimum bactericidal concentration (MBC) values were measured using the microdilution method, and the anti-biofilm activity of the synthetic material was also assessed.

Results: The results demonstrated the inhibitory effects of the synthesized nanoparticles on gram-positive bacteria, with significant growth inhibition observed in *S. aureus* and *B. subtilis*, after exposure to CeO_2 NPs.

Conclusion: CeO_2 NPs synthesized by alginate exhibited significant antibacterial effects against Gram-positive bacteria and could disrupt biofilm structure and prevent further biofilm formation. The findings highlight the potential of CeO_2 NPs synthesized by alginate as a novel antibacterial and anti-biofilm therapeutic agent.

Keywords: Nanoparticles, Cerium oxide, Antibacterial effects, Biofilm

Please cite this article as follows: Mousaiyan S, Baharara J, Es-haghi A, Yousefi E. Investigating the antioxidant, antibacterial, and anti-biofilm effects of cerium oxide nanoparticles synthesized by alginate. Avicenna J Med Biochem. 2024; 12(2):98-105. doi:10.34172/ajmb.2518

Background

The development of antibiotic-resistant bacteria has become a severe popular health concern in recent years (1-3). Despite the development of new antibiotics, bacterial infections are increasingly difficult to treat due to the evolution of resistance mechanisms (4,5). As a result, there is growing interest in exploring alternative approaches such as nanotechnology to combat bacterial infections (6-8).

Nanoparticles have gained increasing attention as a promising alternative to traditional physicochemical methods for fighting pathogenic microorganisms (9-12). The effects of nanoparticles depend on their concentration, composition, size, and chemical and physical properties. Other influencing factors include the source plant species, the plant's growth stage, and the method of fabrication (13-15). Although bulk materials exhibit constant physical properties, this is not true at the nanoscale. Size-dependent properties such as quantum confinement in semiconductor particles, surface plasmon resonance in some metallic particles, and superparamagnetization in magnetic materials have been detected (16-19). During green synthesis, living organisms such as plants, algae, and bacteria, as well as their ingredients are utilized as reducing agents to prepare nanoparticles. Microorganisms, in particular, are among common sources due to their high environmental compatibility, lower energy consumption, and cost-effectiveness (20-23). Microorganisms can carry out their vital processes independently of organic substances and minerals as energy resources. These organisms exhibit high resistance to metals, and when they are exposed to metal ions, they can facilitate the generation of nanoparticles. Metal nanoparticles possess unique physical and chemical properties that make them valuable bioactive agents in medicine, with applications

in optics, catalysts, and antimicrobial therapies (24-26). Cerium oxide (CeO_2, also known as ceria) is a metal oxide belonging to the lanthanide group, which can exhibit two oxidation states, cerium (III) and cerium (IV), in a single cycle due to its high oxidation-reduction potential. Alginate, a polysaccharide composed of α-L-guluronic acid (G) and β-D-mannuronic acid (M) units linked by α1→4 bonds, exists in various sequential arrays such as MMMMM, GGGGG, and MGMGMG. In recent years, alginate has been widely used for storing and transferring various drugs and bio-molecules in medicine (27-29). Cerium oxide nanoparticles (CeO_2 NPs) have emerged as a promising candidate for biomedical applications due to their unique properties, including high antioxidant activity, which allows to effectively scavenge reactive oxygen species (ROS) (30-33). Additionally, CeO_2 NPs have displayed antibacterial and anti-biofilm properties, making them attractive alternatives to conventional antibiotics, especially against antibiotic-resistant pathogenic bacterial strains (34). The mechanism of action of CeO_2 NPs is thought to involve the induction of oxidative stress in the cell membrane components of microorganisms. During this process, a valence change occurs on the surface of CeO_2 NPs, where Ce^{4+} is reduced to Ce^{3+} by gaining an electron (35,36). In the present study, we utilized alginate to synthesize CeO_2 NPs and investigate their antimicrobial properties.

Materials and Methods

Materials

1,1-Diphenyl-2-picrylhydrazyl (DPPH) and butylated hydroxyanisole (BHA) were purchased from Sigma Chemicals Co. (St. Louis, MO, USA). Chloramphenicol antibiotic was obtained from Padtan Teb (Iran), ethanol from Taghtir Khorasan (Iran), and safranin from Daya Exir (Iran). Other reagents were obtained from Merck (Germany). All materials with a purity of 95% or higher were used.

Synthesis of Cerium Oxide Nanoparticles

$Ce(NO_3)_3.6H_2O$ was reacted with alginate sodium (200 mL). In the next step, the CeO_2-alginate mixture was dried at 100 ˚C, and finally, the purified synthesized CeO_2 NPs were obtained by heating the mixture to 450 ˚C, and brownish-color pellets were collected after the synthesis process.

Measurement of Antioxidant Activity of Cerium Oxide Nanoparticles

The antioxidant activity of biosynthesized CeO_2 NPs was measured using the DPPH assay (20). To perform this experiment, 1 mg of DPPH powder was dissolved in 16.9 mL of ethanol, and the resulting solution was kept in a dark place for 30 minutes. Different concentrations of CeO_2 NPs were then added to ethanolic DPPH solution in equal volumes. After incubation for 30 minutes at room temperature, the absorbance of the samples was measured at 517 nm. In this experiment, BHA was used as a standard antioxidant material. All tests were conducted in triplicate.

Kirby-Bauer Disc Diffusion Assay

All experiments were performed in triplicate using Gram-negative *(Escherichia coli* ATCC 25922 and *Pseudomonas aeruginosa* ATCC 9027) and Gram-positive (*Bacillus subtilis* ATCC 1365 and *Staphylococcus aureus* ATCC 25923) bacteria strains (Persian Type Culture Collection, Iran). Blank discs were loaded with CeO_2 NPs at a dose of 300 µg/mL. A bacterial suspension ($OD_{620} = 0.01$) was equally cultured on Muller-Hinton agar medium (Merck, Germany). Antibiotic discs and discs soaked in distilled water were placed on the plate as positive and negative controls, respectively. The plates were incubated at 37 ˚C in for 24 hours. After this period, the inhibition zone around each disc was measured using a ruler (37).

Determination of Minimum Inhibitory Concentration and Minimum Bactericidal Concentration

The micro broth dilution method was used to determine the minimum inhibitory concentration (MIC) and minimum bactericidal concentration (MBC). In this method, a 24-well microplate (SPL Life Sciences, China) was used to prepare various nanoparticle concentrations (0, 25, 50, 75, 100, 125, and 300 µg/mL). The microplate was then placed in an incubator (ParsAzma, Iran) for 24 hours at 37 ˚C. Chloramphenicol antibiotic (Padtan Teb, Iran) was used as a positive control. The first well in which no growing was observed was designated as the MIC.

For MBC determination, wells containing nutrient agar were inoculated with bacteria showing no growth in the previous step. The plate was then incubated at 37˚C for 24 hours. Colony formation confirmed the viability of bacteria, while the absence of colony growth indicated that the bacteria were killed at that concentration (i.e., MBC) (38). All experiments were performed in triplicate. The MBC/MIC ratio was also calculated as a marker of antibacterial activity. An MBC/MIC ratio of ≤ 4 is indicative of a bactericidal agent, while an MBC/MIC ratio > 4 suggests that the agent is bacteriostatic (39).

Investigating Biofilm Generation and Anti-biofilm Effects of Cerium Oxide Nanoparticles

The capacity of biofilm formation by each bacterial strain (*B. subtilis*, *S. aureus*, *E. coli*, and *P. aeruginosa*) was determined using a modified microtiter plate method. First, 180 µL of Tryptone Soy Broth (TSB) medium (Merck, Germany) was added to each well of a 96-well microplate, followed by 10 µL of sterile distilled water in each well. Then, 10 µL of the bacterial suspension was added to each well so that the final volume in each well reached 200 µL. The first wells, which contained only TSB culture medium (200 µL) without bacteria, served as the negative control. Then, the microplate was incubated at 37 ˚C for 48 hours. Afterward, the content of microplates

was discarded, and the wells were washed three times with deionized water. Then, 200 µL of 95% ethanol (Taghtir Khorasan, Iran) was added to each well for 15 minutes to stabilize the biofilm, followed by 200 µL of 0.025% safranin (Daya Exir, Iran) applied for 10 minutes to stain the biofilm. The supernatant was discarded, and the microplate was washed three times with deionized water and allowed to be dried. Finally, the content of each well was dissolved in 200 µL of 33% glacial acetic acid (Merck, Germany), and after 15 minutes, the absorbance of the wells was measured at 492 nm (40).

The modified microtiter plate method was also used to examine the anti-biofilm properties of CeO_2 NPs against *B. subtilis*, *S. aureus*, *E. coli*, and *P. aeruginosa*. First, 180 µL of TSB culture was added to all wells, followed by 10 µL of CeO_2 NPs in each well. Subsequently, 10 µL of the bacterial suspension was added to each well. For the negative control, the wells in the first row of the microplate were enriched with TSB medium (180 µL), bacterial suspension (10 µL), and distilled water (10 µL). The blank well contained only 200 µL of TSB culture medium. Afterward, the microplate was incubated at 37 ˚C for 24 hours. The fixation and staining of bacteria were carried out as described in the previous section (40).

Effects of Cerium Oxide Nanoparticles on Pre-formed Biofilm

To investigate the effects of CeO_2 NPs on pre-formed biofilm, 10 µL of the bacterial and 180 µL of TSB medium were mixed and added to all wells of a 96-well microplate. After 24 hours incubation at 37 ˚C, the microplate was removed, and 10 µL of CeO_2 NPs were added to each well, resulting in final concentrations of 0, 25, 50, 75, 100, 125, and 300 µg/mL. After three hours of additional incubation, the contents of the wells were withdrawn, and the wells were washed with distilled water. Ethanol and safranin were used for fixation and staining, respectively, as discussed previously. The dye was solved in acetic acid, and its absorbance was recorded by enzyme-linked immunosorbent assay (ELISA) reader (BioRad, USA) at 492 nm. The biofilm inhibition percentage was calculated using the following formula (41):

Percentage inhibition of biofilm formation = [[OD492 positive control / OD492 biocide] × 100] - 100

Statistical Analysis

All experiments were performed in triplicate, and the results were analyzed using SPSS software and the ANOVA test. A P value of < 0.05 was considered statistically significant. The data are presented as mean ± standard deviation.

Results

Antioxidant Activity Assay

The antioxidant capacity of biosynthesized CeO_2 NP was assessed by evaluating their free radical scavenging activity using DPPH assay (Figure 1). The data from the DPPH assay confirmed that the CeO_2 NPs synthesized by alginate can remove free radicals significantly ($P < 0.001$). The CeO_2 NP inhibited the DPPH free radicals in a dose-dependent manner, with an IC_{50} value of 125 µg/mL, indicating the concentration at which 50% of free radicals were scavenged.

The Finding of Disc Diffusion Assay

The diameters of the non-growth halo of *S. aureus* and *B. subtilis* exposed to CeO_2 NPs synthesized by alginate were 13.33 ± 0.1 and 12.66 ± 0.1 mm, respectively. However, *E. coli* and *P. aeruginosa* were resistant to nanoparticles, and no halo zone was formed around the discs (Figure 2 and Table 1).

Minimum Bactericidal Concentration and Minimum Inhibitory Concentration Results

The average MICs of CeO_2 NPs synthesized by alginate for

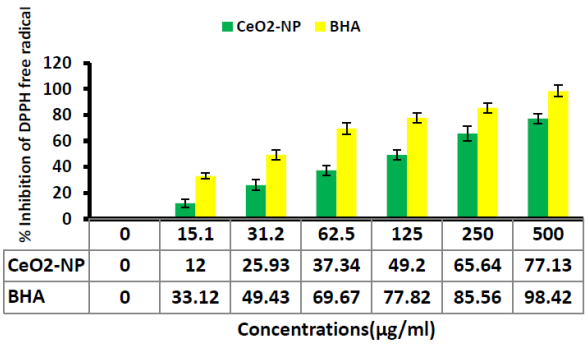

	0	15.1	31.2	62.5	125	250	500
CeO2-NP	0	12	25.93	37.34	49.2	65.64	77.13
BHA	0	33.12	49.43	69.67	77.82	85.56	98.42

Figure 1. Anti-oxidant Activity of CeO_2 NPs Synthesized by Alginate Using DPPH Assay. *Note.* CeO2 NPs: Cerium oxide nanoparticles; DPPH: 1,1-Diphenyl-2-picrylhydrazyl. BHA was used as a standard antioxidant in this experiment

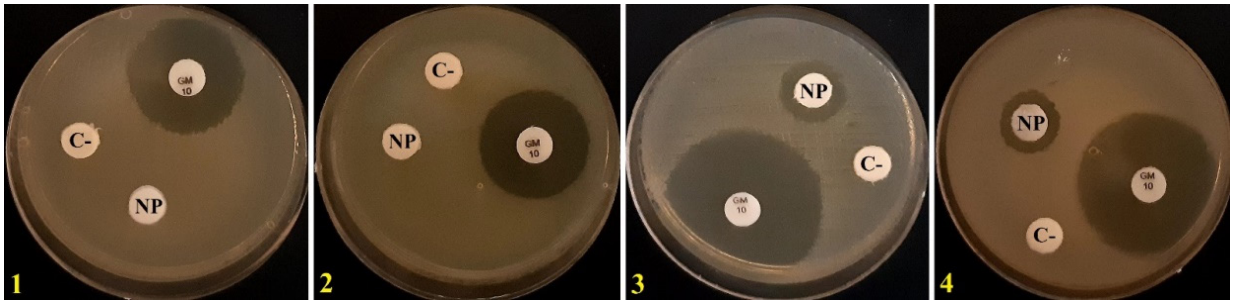

Figure 2. Disk Diffusion Assay. *Note.* NP: CeO_2 NPs synthesized by alginate; C-: Negative control; GM: Gentamicin; 1: *Escherichia coli,* 2: *Pseudomonas aeruginosa;* 3: *Staphylococcus aureus;* 4: *Bacillus subtilis*

S. aureus and *B. subtilis* were 125 ± 00 and 150 ± 00 µg/mL, respectively, while the MBCs were 175 ± 00 and 175 ± 00 µg/mL, respectively. There was no significant difference between the MIC of CeO_2 NPs synthesized by alginate and chloramphenicol against *B. subtilis* and *S. aureus* ($P < 0.5$). The MBC/MIC ratio is presented in Table 2.

The MBC/MIC ratio indicated that CeO_2 NPs synthesized by alginate exhibit bactericidal activity against *B. subtilis* and *S. aureus*.

Investigation of Biofilm Formation

The phenotypic examination of biofilm formation by the titration microplate method exhibits that *B. subtilis*, *S. aureus*, *E. coli*, and *P. aeruginosa* establish strong biofilm. As shown in Table 3, all bacterial strains (i.e., *B. subtilis*, *S. aureus*, *E. coli*, and *P. aeruginosa*) could form strong biofilms.

Effects of Cerium Oxide Nanoparticles on Biofilm Inhibition

Biofilm generation was evaluated in the various concentrations of CeO_2 NPs. The average absorption at 492 nm was calculated after three repetitions to assess the nanoparticles' capacity to inhibit biofilm formation. The results showed that light absorption inversely correlated with the concentration of nanoparticles, in contrast to the positive control, indicating a reduction in biofilm formation in the presence of CeO_2 NPs.

As observed in Figure 2, biofilm formation decreased with increasing concentrations of CeO_2 NPs, as evidenced by a decline in absorbance. This indicates a lower biofilm formation activity at higher concentrations of CeO NPs. Moreover, after complete inhibition of biofilm formation at certain concentrations, absorption slightly increased compared to the control, but this increase was not statistically significant and could be attributed to the presence of nanoparticles. According to Figure 3, the biofilm inhibitory effects of CeO_2 NPs for *B. subtilis* and *S. aureus* were similar; however, CeO_2 NPs had no significant anti-biofilm effects on *E. coli* and *P. aeruginosa*.

According to Figure 3, CeO_2 NPs could not remove biofilm already made by Gram-negative strains. However, at elevated concentrations, CeO_2 NPs could remove the biofilm formed by Gram-positive strains. As shown in Figure 3, from the minimal biofilm-eradicating concentration downward, light absorption slightly increased compared to the control, which could be due to the presence of nanoparticles. As illustrated in Figure 4, at the same concentration, CeO_2 NPs were more effective in removing biofilm formed by *B. subtilis* compared to *S. aureus*.

Discussion

In recent years, some notable developments have emerged in nanotechnology, highlighting the applications of

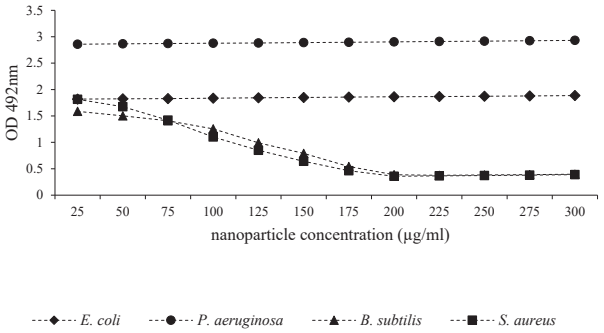

Figure 3. The Effect of CeO_2 NPs on the Reduction of Biofilm Formation.
Note. CeO_2 NPs: Cerium nanoparticles

Table 1. Results Obtained From Disk Diffusion Test

Material	*Escherichia coli* ATCC 8739	*Pseudomonas aeruginosa* ATCC 9027	*Staphylococcus aureus* ATCC 6538	*Bacillus subtilis* ATCC 6633
Nanoparticle (300 µg/mL)	-	-	13.33 ± 0.1 mm	12.77 ± 0.1 mm
Gentamicin (10 µg) [positive control]	21 ± 0.2 mm	20.62 ± 0.1 mm	29 ± 0.2 mm	25.56 ± 0.3 mm

Note. –: No activity.
The diameter of the reticence zone was dignified with a ruler, and the data were reported in millimeters (mm).

Table 2. MIC, MBC, and MBC/MIC Ratios of CeO_2 NPs Produced by Alginate (µg/mL) Against 4 ATCC Bacteria

Bacteria	CeO_2 NPs			Chloramphenicol		
	MIC (mg/mL)	MBC (mg/mL)	MBC/MIC ratio	MIC (µg/mL)	MBC (µg/mL)	MBC/MIC Ratio
Escherichia coli ATCC 8739	-	-	-	75 ± 00	100 ± 00	1.33 (+)
Pseudomonas aeruginosa ATCC 9027	-	-	-	100 ± 00	125 ± 00	1.25 (+)
Staphylococcus aureus ATCC 6538	125 ± 00	175 ± 00	1.4 (+)	100 ± 00	125 ± 00	1.25 (+)
Bacillus subtilis ATCC 6633	150 ± 00	175 ± 00	1.16 (+)	100 ± 00	100 ± 00	1 (+)

Note. CeO_2 NPs: Cerium oxide nanoparticles; MBC: Minimum bactericidal concentration; MIC: Minimum inhibitory concentration; (+): Bactericidal; –: No activity.

Table 3. Optical Absorption (OD_{492}) of 4 ATCC Bacterial Strains Forming Biofilms Over 48 Hours

Bacterial Strains and Control	*Escherichia coli* ATCC 25922	*Pseudomonas aeruginosa* ATCC 9027	*Bacillus subtilis* PTCC 1365	*Staphylococcus aureus* ATCC 25923	Control
Mean	2.103 ± 0.0011	2.593 ± 0.0013	1.711 ± 0.0009	1.867 ± 0.0015	0.338

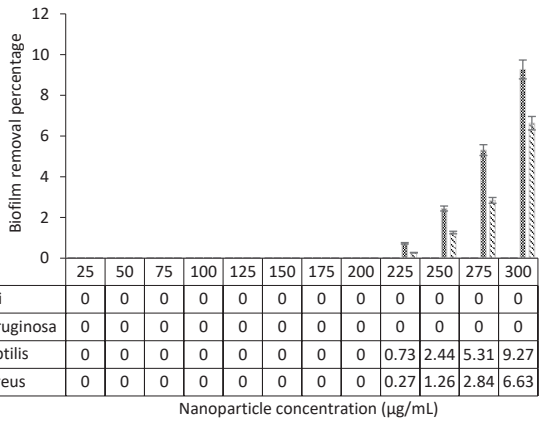

	25	50	75	100	125	150	175	200	225	250	275	300
E. coli	0	0	0	0	0	0	0	0	0	0	0	0
P. aeruginosa	0	0	0	0	0	0	0	0	0	0	0	0
B. subtilis	0	0	0	0	0	0	0	0	0.73	2.44	5.31	9.27
S. aureus	0	0	0	0	0	0	0	0	0.27	1.26	2.84	6.63

Figure 4. The Percentage of Removal of Biofilm Formed in the Presence of Various Concentrations of CeO_2 NPs. *Note.* CeO_2 NPs: Cerium nanoparticles

nanoparticles in many areas, especially in medicine (42-44). Nanomaterials with anti-bacterial and anti-fungal properties are useful not only in medicine but also in food preservation and packaging. In metal oxide nanoparticles, CeO_2 has received greater attention due to its distinctive effects such as free radical cleaning activity and a broad range of other features (45,46). The biomedical applications of ceria nanoparticles seem quite promising, and research has highlighted their potential use as therapeutic agents to combat diseases characterized by excessive free radical generation and oxidative stress (47-50). The experiments in this study demonstrated that CeO_2 NPs synthesized by alginate successfully slowed the growth of Gram-positive bacteria. Furthermore, the nanoparticles demonstrated anti-biofilm formation activity, effectively reducing biofilm production by these bacterial species.

The antibacterial and anti-biofilm properties of CeO_2 NPs have been extensively studied in recent years. However, the synthesis of CeO_2 NPs using natural polymers such as alginate is a relatively new approach that offers several advantages over traditional methods (51,52). In this research, we demonstrated the antibacterial and anti-biofilm activity of CeO_2 NPs produced by alginate.

In this study, the antibacterial efficacy of CeO_2 NPs synthesized via alginate was observed against both Gram-positive and Gram-negative bacterial strains. The nanoparticles likely exerted their antibacterial effect through multiple mechanisms, including the generation of ROS, disruption of bacterial cell membranes, and interaction with bacterial enzymes and DNA. The unique surface properties of CeO_2 NPs, facilitated by alginate stabilization, might enhance their interaction with bacterial cells. Furthermore, alginate, known for its inherent antimicrobial properties, could synergize with the nanoparticles to boost antibacterial activity. This dual effect suggests that CeO_2 NPs synthesized with alginate are potentially effective antibacterial agents against both Gram-positive and Gram-negative bacteria.

Biofilm formation is a critical factor in chronic infections, and traditional antibacterial agents often fail to penetrate biofilms effectively. CeO_2 NPs synthesized using alginate demonstrated promising anti-biofilm properties, likely due to their ability to disrupt biofilm matrix integrity and inhibit bacterial adhesion. The anti-biofilm mechanism could involve the nanoparticles interfering with quorum sensing, a communication process essential for biofilm development. Additionally, ROS generation by the nanoparticles may disrupt biofilm structure and inhibit bacterial growth within biofilms. The biocompatibility and non-toxic nature of alginate further enhance the appeal of this approach for preventing biofilm-associated infections (53-55).

Importantly, the CeO_2 NPs synthesized by alginate were found to be non-toxic to human cells, indicating their plausible safety for medical applications. Furthermore, the alginate-mediated synthetic method used in the current study offers a cost-effective and environment-friendly way of producing these nanoparticles, making them an attractive alternative that warrants further development and testing. The strong antibacterial and anti-biofilm activity of CeO_2 NPs synthesized by alginate can be of particular interest to microbiologists and specialists in infectious diseases, as well as professionals in other medicinal fields. For example, CeO_2 NPs synthesized by alginate can be used as coatings for medical implants to prevent bacterial colonization and reduce the risk of implant-related infections. These nanoparticles can also be incorporated into wound dressings to promote wound healing and prevent bacterial infections (56,57). Moreover, CeO_2 NPs can be employed as drug delivery systems, providing targeted delivery of antimicrobial agents to bacterial cells. Overall, given that nanoparticles have a high surface area-to-volume ratio, they form an ideal system for drug delivery.

Conclusion

The results of this study revealed that CeO_2 NPs synthesized by alginate have significant antibacterial activity against Gram-positive bacteria. This antibacterial capacity was dose-dependent, with higher concentrations of CeO_2 NPs leading to greater inhibition of bacterial growth. Furthermore, CeO_2 NPs exhibited significant anti-biofilm activity against *S. aureus* and *B. subtilis*. Biofilms are problematic for their role in bacterial resistance to antibiotics and other antimicrobial agents, making infections caused by these microorganisms difficult to treat. However, CeO_2 NPs synthesized by alginate in this study were effective in disrupting biofilm structure and preventing further biofilm formation. The findings demonstrated the significant potential of CeO_2 NPs synthesized by alginate as a potential novel antibacterial and anti-biofilm therapeutic agent. Further research is required to assess the safety and effectiveness of these nanoparticles *in vivo* and to assess their applicability to be used in clinical settings.

Acknowledgments

The authors appreciate Islamic Azad University, Mashhad Branch, for their support and assistance.

Authors' Contribution

Conceptualization: Soudabe Mousaiyan, Javad Baharara, Ali Es-haghi.
Data curation: Soudabe Mousaiyan, Javad Baharara, Ali Es-haghi.
Formal analysis: Soudabe Mousaiyan, Javad Baharara, Ali Es-haghi.
Investigation: Soudabe Mousaiyan, Javad Baharara, Ali Es-haghi, Ehsan Yousefi.
Methodology: Soudabe Mousaiyan, Javad Baharara, Ali Es-haghi, Ehsan Yousefi.
Project administration: Ali Es-haghi.
Resources: Ali Es-haghi.
Software: Ali Es-haghi, Ehsan Yousefi.
Supervision: Ali Es-haghi.
Validation: Ali Es-haghi.
Visualization: Javad Baharara, Ali Es-haghi.
Writing–original draft: Soudabe Mousaiyan, Javad Baharara, Ali Es-haghi, Ehsan Yousefi.
Writing–review & editing: Ali Es-haghi.

Competing Interests

The authors declare no conflict of interests.

Ethical Approval

Not applicable.

Funding

None.

References

1. Bagherian MS, Zargham P, Zarharan H, Bakhtiari M, Mortezaee Ghariyeh Ali N, Yousefi E, et al. Antimicrobial and antibiofilm properties of selenium-chitosan-loaded salicylic acid nanoparticles for the removal of emerging contaminants from bacterial pathogens. World J Microbiol Biotechnol. 2024;40(3):86. doi: 10.1007/s11274-024-03917-z.
2. Rezaei MR, Es-Haghi A, Yaghmaei P, Ghobeh M. Assessment of antioxidant and antimicrobial activities of silver nanoparticles biosynthesized by *Haplophyllum obtusifolium*. 2020;8(2):94-8. doi: 10.34172/ajmb.2020.14.
3. Amiri MS, Taghavizadeh Yazdi ME, Rahnama M. Medicinal plants and phytotherapy in Iran: glorious history, current status and future prospects. Plant Sci Today. 2021;8(1):95-111. doi: 10.14719/pst.2021.8.1.926.
4. Mancuso G, Midiri A, Gerace E, Biondo C. Bacterial antibiotic resistance: the most critical pathogens. Pathogens. 2021;10(10):1310. doi: 10.3390/pathogens10101310.
5. 5.Mousavi-Kouhi SM, Beyk-Khormizi A, Amiri MS, Mashreghi M, Taghavizadeh Yazdi ME. Silver-zinc oxide nanocomposite: from synthesis to antimicrobial and anticancer properties. Ceram Int. 2021;47(15):21490-7. doi: 10.1016/j.ceramint.2021.04.160.
6. Ozdal M, Gurkok S. Recent advances in nanoparticles as antibacterial agent. ADMET DMPK. 2022;10(2):115-29. doi: 10.5599/admet.1172.
7. Es-Haghi A, Amiri MS, Taghavizadeh Yazdi ME. Ferula latisecta gels for synthesis of zinc/silver binary nanoparticles: antibacterial effects against gram-negative and gram-positive bacteria and physicochemical characteristics. BMC Biotechnol. 2024;24(1):51. doi: 10.1186/s12896-024-00878-x.
8. Mohammadzadeh V, Rahiman N, Cabral H, Quader S, Zirak MR, Taghavizadeh Yazdi ME, et al. Poly-γ-glutamic acid nanoparticles as adjuvant and antigen carrier system for cancer vaccination. J Control Release. 2023;362:278-96. doi: 10.1016/j.jconrel.2023.08.049.
9. Taghavizadeh Yazdi ME, Hamidi A, Amiri MS, Kazemi Oskuee R, Hosseini HA, Hashemzadeh A, et al. Eco-friendly and plant-based synthesis of silver nanoparticles using *Allium giganteum* and investigation of its bactericidal, cytotoxicity, and photocatalytic effects. Mater Technol. 2019;34(8):490-7. doi: 10667857.2019.1583408.
10. Taghavizadeh Yazdi ME, Qayoomian M, Beigoli S, Boskabady MH. Recent advances in nanoparticle applications in respiratory disorders: a review. Front Pharmacol. 2023;14:1059343. doi: 10.3389/fphar.2023.1059343.
11. Nateq Golestan M, Abbasi MR, Rakhshandeh H, Taghavizadeh Yazdi ME. Facile fabrication and characterization of silver nanoparticles by sunn pest (*Eurygaster integriceps* Puton) damaged wheat and evaluation of its antibacterial and cellular toxicity toward liver cancer cell lines. Studies in Medical Sciences. 2023;34(10):586-97. doi: 10.61186/umj.34.10.586.
12. Zarharan H, Bagherian M, Shah Rokhi A, Ramezani Bajgiran R, Yousefi E, Heravian P, et al. The anti-angiogenesis and antioxidant activity of chitosan-mediated synthesized selenium-gold nanostructure. Arab J Chem. 2023;16(7):104806. doi: 10.1016/j.arabjc.2023.104806.
13. Halimi Khalil Abad M, Nadaf M, Taghavizadeh Yazdi ME. Biosynthesis of ZnO.Ag2O3 using aqueous extract of *Haplophyllum obtusifolium*: characterization and cell toxicity activity against liver carcinoma cells. Micro Nano Lett. 2023;18(6):e12170. doi: 10.1049/mna2.12170.
14. Hamidi A, Taghavizadeh Yazdi ME, Amiri MS, Hosseini HA, Darroudi M. Biological synthesis of silver nanoparticles in *Tribulus terrestris* L. extract and evaluation of their photocatalyst, antibacterial, and cytotoxicity effects. Res Chem Intermed. 2019;45(5):2915-25. doi: 10.1007/s11164-019-03770-y.
15. Rahimi E, Asefi F, Afzalinia A, Khezri S, Zare-Zardini H, Ghorani-Azam A, et al. Chitosan coated copper/silver oxide nanoparticles as carriers of breast anticancer drug: cyclin D1/P53 expressions and cytotoxicity studies. Inorg Chem Commun. 2023;158:111581. doi: 10.1016/j.inoche.2023.111581.
16. Lian F, Xing B. From bulk to nano: formation, features, and functions of nano-black carbon in biogeochemical processes. Environ Sci Technol. 2024;58(36):15910-25. doi: 10.1021/acs.est.4c07027.
17. Xue J, Wang R, Yang Y. The surface of halide perovskites from nano to bulk. Nat Rev Mater. 2020;5(11):809-27. doi: 10.1038/s41578-020-0221-1.
18. Petracic O. Superparamagnetic nanoparticle ensembles. Superlattices Microstruct. 2010;47(5):569-78. doi: 10.1016/j.spmi.2010.01.009.
19. Taghavizadeh Yazdi ME, Khara J, Sadeghnia HR, Esmaeilzadeh Bahabadi S, Darroudi M. Biosynthesis, characterization, and antibacterial activity of silver nanoparticles using *Rheum turkestanicum* shoots extract. Res Chem Intermed. 2018;44(2):1325-34. doi: 10.1007/s11164-017-3169-z.
20. Taghavizadeh Yazdi ME, Housaindokht MR, Sadeghnia HR, Esmaeilzadeh Bahabadi S, Amiri MS, Darroudi M. Assessment of phytochemical components and antioxidant activity of *Rheum turkestanicum* Janisch. Studies in Medical Sciences. 2020;31(2):75-81.
21. Ashna M, Es-Haghi A, Karimi Noghondar M, Al Amara D, Taghavizadeh Yazdi ME. Greener synthesis of cerium oxide nanoemulsion using pollen grains of *Brassica napus* and evaluation of its antitumour and cytotoxicity properties. Mater Technol. 2022;37(8):525-32. doi: 10.1080/10667857.2020.1863558.
22. Darroudi M, Taghavizadeh Yazdi ME, Amiri MS. Plant-mediated biosynthesis of nanoparticles. In: 21st Century Nanoscience–A Handbook. CRC Press; 2020.
23. Shakerimanesh K, Bayat F, Shahrokhi A, Baradaran A, Yousefi E, Mashreghi M, et al. Biomimetic synthesis and characterisation of homogenouse gold nanoparticles and estimation of its cytotoxity against breast cancer cell line. Mater Technol. 2022;37(13):2853-60. doi:

10.1080/10667857.2022.2081287.
24. Es-Haghi A, Javadi F, Taghavizadeh Yazdi ME, Amiri MS. The expression of antioxidant genes and cytotoxicity of biosynthesized cerium oxide nanoparticles against hepatic carcinoma cell line. 2019;7(1):16-20. doi: 10.34172/ajmb.2019.04.
25. Es-Haghi A, Taghavizadeh Yazdi ME, Sharifalhoseini M, Baghani M, Yousefi E, Rahdar A, et al. Application of response surface methodology for optimizing the therapeutic activity of ZnO nanoparticles biosynthesized from *Aspergillus niger*. Biomimetics (Basel). 2021;6(2):34. doi: 10.3390/biomimetics6020034.
26. Ahmadi R, Es-Haghi A, Zare-Zardini H, Taghavizadeh Yazdi ME. Nickel oxide nanoparticles synthesized by rose hip extract exert cytotoxicity against the HT-29 colon cancer cell line through the caspase-3/caspase-9/Bax pathway. Emergent Mater. 2023;6(6):1877-88. doi: 10.1007/s42247-023-00572-2.
27. Abnoos M, Mohseni M, Mousavi SA, Ashtari K, Ilka R, Mehravi B. Chitosan-alginate nano-carrier for transdermal delivery of pirfenidone in idiopathic pulmonary fibrosis. Int J Biol Macromol. 2018;118(Pt A):1319-25. doi: 10.1016/j.ijbiomac.2018.04.147.
28. Feyissa Z, Edossa GD, Gupta NK, Negera D. Development of double crosslinked sodium alginate/chitosan-based hydrogels for controlled release of metronidazole and its antibacterial activity. Heliyon. 2023;9(9):e20144. doi: 10.1016/j.heliyon.2023.e20144.
29. Hashemzadeh V, Hashemzadeh A, Mohebbati R, Gharari Arefi R, Taghavizadeh Yazdi ME. Fabrication and characterization of gold nanoparticles using alginate: in vitro and in vivo assessment of its administration effects with swimming exercise on diabetic rats. Open Life Sci. 2024;19(1):20220869. doi: 10.1515/biol-2022-0869.
30. Saifi MA, Seal S, Godugu C. Nanoceria, the versatile nanoparticles: promising biomedical applications. J Control Release. 2021;338:164-89. doi: 10.1016/j.jconrel.2021.08.033.
31. Alabyadh T, Albadri R, Es-Haghi A, Taghavizadeh Yazdi ME, Ajalli N, et al. ZnO/CeO2 nanocomposites: metal-organic framework-mediated synthesis, characterization, and estimation of cellular toxicity toward liver cancer cells. J Funct Biomater. 2022;13(3):139. doi: 10.3390/jfb13030139.
32. Ghorani-Azam A, Mottaghipisheh J, Amiri MS, Mashreghi M, Hashemzadeh A, Haddad-Mashadrizeh A, et al. Resveratrol-mediated gold-nanoceria synthesis as green nanomedicine for phytotherapy of hepatocellular carcinoma. Front Biosci (Landmark Ed). 2022;27(8):227. doi: 10.31083/j.fbl2708227.
33. Farhangi MJ, Es-Haghi A, Taghavizadeh Yazdi ME, Rahdar A, Baino F. MOF-mediated synthesis of CuO/CeO2 composite nanoparticles: characterization and estimation of the cellular toxicity against breast cancer cell line (MCF-7). J Funct Biomater. 2021;12(4):53. doi: 10.3390/jfb12040053.
34. Uzair B, Akhtar N, Sajjad S, Bano A, Fasim F, Zafar N, et al. Targeting microbial biofilms: by *Arctium lappa* L. synthesised biocompatible CeO2-NPs encapsulated in nano-chitosan. IET Nanobiotechnol. 2020;14(3):217-23. doi: 10.1049/iet-nbt.2019.0294.
35. Farias IA, Dos Santos CC, Sampaio FC. Antimicrobial activity of cerium oxide nanoparticles on opportunistic microorganisms: a systematic review. Biomed Res Int. 2018;2018:1923606. doi: 10.1155/2018/1923606.
36. Nadeem M, Khan R, Afridi K, Nadhman A, Ullah S, Faisal S, et al. Green synthesis of cerium oxide nanoparticles (CeO2 NPs) and their antimicrobial applications: a review. Int J Nanomedicine. 2020;15:5951-61. doi: 10.2147/ijn.S255784.
37. Taghavizadeh Yazdi ME, Darroudi M, Amiri MS, Zarrinfar H, Hosseini HA, Mashreghi M, et al. Antimycobacterial, anticancer, antioxidant and photocatalytic activity of biosynthesized silver nanoparticles using berberis integerrima. Iran J Sci Technol Trans A Sci. 2022;46(1):1-11. doi: 10.1007/s40995-021-01226-w.
38. Najafi M, Nakhaei Moghaddam M, Yousefi E. The effect of silver nanoparticles on pyocyanin production of *Pseudomonas aeruginosa* isolated from clinical specimens. Avicenna J Med Biotechnol. 2021;13(2):98-103. doi: 10.18502/ajmb.v13i2.5529.
39. Mogana R, Adhikari A, Tzar MN, Ramliza R, Wiart C. Antibacterial activities of the extracts, fractions and isolated compounds from *Canarium patentinervium* Miq. against bacterial clinical isolates. BMC Complement Med Ther. 2020;20(1):55. doi: 10.1186/s12906-020-2837-5.
40. Zhang H, Cheng J, Ao Q. Preparation of alginate-based biomaterials and their applications in biomedicine. Mar Drugs. 2021;19(5):264. doi: 10.3390/md19050264.
41. Gobi R, Ravichandiran P, Babu RS, Yoo DJ. Biopolymer and synthetic polymer-based nanocomposites in wound dressing applications: a review. Polymers (Basel). 2021;13(12):1962. doi: 10.3390/polym13121962.
42. Momen Eslamieh-Ei F, Sharifi Moghaddam Mood N, Amin Poustchi Tousi S, Basharkhah S, Mottaghipisheh J, Es-Haghi A, et al. Synthesis and its characterisation of selenium/silver/chitosan and cellular toxicity against liver carcinoma cells studies. Nat Prod Res. 2023:1-9. doi: 10.1080/14786419.2023.2256023.
43. Hashemzadeh MR, Taghavizadeh Yazdi ME, Amiri MS, Mousavi SH. Stem cell therapy in the heart: biomaterials as a key route. Tissue Cell. 2021;71:101504. doi: 10.1016/j.tice.2021.101504.
44. Moshirian Farahi SM, Taghavizadeh Yazdi ME, Einafshar E, Akhondi M, Ebadi M, Azimipour S, et al. The effects of titanium dioxide (TiO2) nanoparticles on physiological, biochemical, and antioxidant properties of *Vitex* plant (*Vitex agnus - Castus* L). Heliyon. 2023;9(11):e22144. doi: 10.1016/j.heliyon.2023.e22144.
45. Iqbal N, Anastasiou A, Aslam Z, Raif EM, Do T, Giannoudis PV, et al. Interrelationships between the structural, spectroscopic, and antibacterial properties of nanoscale (<50 nm) cerium oxides. Sci Rep. 2021;11(1):20875. doi: 10.1038/s41598-021-00222-9.
46. Muthuvel A, Jothibas M, Mohana V, Manoharan C. Green synthesis of cerium oxide nanoparticles using *Calotropis procera* flower extract and their photocatalytic degradation and antibacterial activity. Inorg Chem Commun. 2020;119:108086. doi: 10.1016/j.inoche.2020.108086.
47. Javadi F, Taghavizadeh Yazdi ME, Baghani M, Es-Haghi A. Biosynthesis, characterization of cerium oxide nanoparticles using *Ceratonia siliqua* and evaluation of antioxidant and cytotoxicity activities. Mater Res Express. 2019;6(6):065408. doi: 10.1088/2053-1591/ab08ff.
48. Al Khafaji SJS, Ghobeh M, Mashergi M, Es-Haghi A. Biological synthesis of cerium oxide nanoparticles using funnel extract: characterization and evaluation of its angiogenesis and cytotoxicity properties against breast cancer cells. Bionanoscience. 2024. doi: 10.1007/s12668-024-01355-7.
49. Aseyd Nezhad S, Es-Haghi A, Homayouni Tabrizi M. Green synthesis of cerium oxide nanoparticle using *Origanum majorana* L. leaf extract, its characterization and biological activities. Appl Organomet Chem. 2020;34(2):e5314. doi: 10.1002/aoc.5314.
50. Mousaiyan S, Baharara J, Es-haghi A. Biopreparation of cerium oxide nanoparticles using alginate: characterization and estimation of antioxidant and its activity against breast cancer cell lines (MCF7). Results Chem. 2024;7:101468. doi: 10.1016/j.rechem.2024.101468.
51. Shalini ASS, Shahanaz L, Rajeswaran P, Tamilarasan R, Kumaran S, Karthik PS. Facile green synthesis of gelatin sodium

alginate cerium oxide hydrogel nanocomposite and their photocatalytic and its biological applications. Chem Zvesti. 2024;78(5):3111-23. doi: 10.1007/s11696-023-03297-y.
52. Das S, Swain S, Rautray TR. Incorporation of hydroxyapatite and cerium oxide nanoparticle scaffold as an antibacterial filler matrix for biomedical applications. Int J Artif Organs. 2024;47(5):356-61. doi: 10.1177/03913988241234548.
53. Kim YG, Lee Y, Lee N, Soh M, Kim D, Hyeon T. Ceria-based therapeutic antioxidants for biomedical applications. Adv Mater. 2024;36(10):e2210819. doi: 10.1002/adma.202210819.
54. Alarfaj N, Al Musayeib N, Amina M, El-Tohamy M. Synthesis and characterization of polysiphonia/cerium oxide/nickel oxide nanocomposites for the removal of toxins from contaminated water and antibacterial potential. Environ Sci Pollut Res Int. 2024;31(11):17064-96. doi: 10.1007/s11356-024-32199-z.
55. Wei Z, Niu Z, Xu H, Li Z, Wang P, Li C, et al. Facile synthesis of a CeMnOx catalytic gel with bacterial microenvironment-responsive antibacterial properties. New J Chem. 2024;48(21):9685-93. doi: 10.1039/d4nj01440e.
56. Almuslem AS, Alshehri AM, Menazea AA, Farea MO, El-Morsy MA. Morphological and biological assessment of films based on hyaluronic acid doped with cerium oxide and aluminum oxide for wound healing applications. Mater Chem Phys. 2024;320:129450. doi: 10.1016/j.matchemphys.2024.129450.
57. Kamalipooya S, Fahimirad S, Abtahi H, Golmohammadi M, Satari M, Dadashpour M, et al. Diabetic wound healing function of PCL/cellulose acetate nanofiber engineered with chitosan/cerium oxide nanoparticles. Int J Pharm. 2024;653:123880. doi: 10.1016/j.ijpharm.2024.123880.